Nanotechnology in Biomaterials

JOURNAL OF biomaterials applications

Journal of Biomaterials Applications
2022, Vol. 36(6) 1098–1110

DOI: 10.1177/08853282211046418
journals.sagepub.com/home/jba
SAGE

Biophysical properties of electrospun chitosan-grafted poly(lactic acid) nanofibrous scaffolds loaded with chondroitin sulfate and silver nanoparticles

Alexandre F Júnior[1], Charlene A Ribeiro[1], Maria E Leyva[2], Paulo S Marques[3], Carlos R J Soares[4] and Alvaro A Alencar de Queiroz[4]

Abstract

The aim of this work was to study the biophysical properties of the chitosan-grafted poly(lactic acid) (CH-g-PLA) nanofibers loaded with silver nanoparticles (AgNPs) and chondroitin-4-sulfate (C_4S). The electrospun CH-g-PLA:AgNP:C_4S nanofibers were manufactured using the electrospinning technique. The microstructure of the CH-g-PLA:AgNP:C_4S nanofibers was investigated by proton nuclear magnetic resonance (^{1}H-NMR), scanning electron microscopy (SEM), UV-Visible spectroscopy (UV-Vis), X-ray diffraction (XRD), and Fourier transform infrared (ATR-FTIR) spectroscopy. ATR-FTIR and ^{1}H-NMR confirm the CH grafting successfully by PLA with a substitution degree of 33.4%. The SEM measurement results indicated apparently smooth nanofibers having a diameter range of 340 ± 18 nm with porosity of 89 ± 3.08% and an average pore area of 0.27 μm^2. UV-Vis and XRD suggest that silver nanoparticles with the size distribution of 30 nm were successfully incorporated into the electrospun nanofibers. The water contact angle of 12.8 ± 2.7° reveals the hydrophilic nature of the CH-g-PLA:AgNP:C_4S nanofibers has been improved by C_4S. The electrospun CH-g-PLA:AgNP:C_4S nanofibers are found to release ions Ag+ at a concentration level capable of rendering an antimicrobial efficacy. Gram-positive bacteria (*S.aureus*) were more sensitive to CH-g-PLA:AgNP:C_4S than Gram-negative bacteria (*E. coli*). The electrospun CH-g-PLA:AgNP:C_4S nanofibers exhibited no cytotoxicity to the L-929 fibroblast cells, suggesting cytocompatibility. Fluorescence microscopy demonstrated that C_4S promotes the adhesion and proliferation of fibroblast cells onto electrospun CH-g-PLA:AgNP:C_4S nanofibers.

Keywords

Electrospun nanofibers, grafted chitosan, poly (lactic acid), chondroitin sulfate, silver nanoparticles

Introduction

Chitosan (CH)-based materials fulfilling various important applications in biomedicine, such as gels for drug reservoirs, scaffolds for tissue engineering, and artificial blood vessels, among others.[1] CH has also received recognition from the Food and Drug Administration (FDA), United States, as a biopolymer that is safe to be applied in the health industry, especially for medicine and food.[2]

Nowadays, CH and its derivatives have gained a great popularity in pharmaceutical industries and become more and more important in this field owing to production of new derivatives and finding new applications for existed compounds by medicine.[2]

CH is a privileged class of biopolymers, which can be easily converted into other substances for many purposes in medicine.[3,4] Recently, a great deal of attention has been devoted to CH grafted with poly(lactic acid) (PLA).[5,6] CH-g-PLA is the esterification product of one carboxyl group of PLA with chitosan, which can be prepared by different

[1]Doctorate Post-graduate scholarship in Materials for Engineering/Biomaterials (CAPES), Federal University of Itajubá (UNIFEI), Itajubá, Brazil
[2]Institute of Physics and Chemistry/Federal University of Itajubá (UNIFEI), Itajubá, Brazil
[3]Institute of Natural Resources (IRN)/Federal University of Itajubá (UNIFEI), Itajubá, Brazil
[4]Biotechnology Center (CEBIO), Nuclear and Energy Research Institute, Sao Paulo, Brazil

Corresponding author:
Alvaro A Alencar de Queiroz, Biotechnology Center (CEBIO), Nuclear and Energy Research Institute (IPEN), Lineu Prestes, 2242, Butantã, São Paulo-SP 05508-000, Brazil.
Email: alvaro.queiroz@ipen.br, dealenquer@gmail.com

chemical routes.[7,8] CH-g-PLA has been demonstrated to be biocompatible and biodegradable in a number of applications in the medical device and pharmaceutical area for either drug or protein delivery systems.[9–12]

Although CH-blended PLA electrospun nanofibers has been reported,[13–16] to the best of our knowledge, there is no report on the production of electrospun CH-g-PLA nanofibers loaded with chondroitin sulfate (C_4S) and silver nanoparticles (AgNPs). The use of electrospun CH-g-PLA nanofibers for biomedical applications has some internal advantages such as deposition in fibrous forms or constructions that mimicking or replicating the extracellular matrix (ECM).

In medicine, the antimicrobial properties of AgNP are used to develop antibacterial materials to control microbial infections in wound healing for a better treatment outcome.[17] AgNP can continually release silver ions that can adhere to the microbial cell wall and cytoplasmic membrane and lead to disruption of the bacterial envelope deactivating the respiratory enzymes, generating reactive oxygen species, and interrupting DNA replication that results in the in termination of the growth of the microorganisms.[18]

Chondroitin sulfate (C_4S) is an important sulfated polyssachariде component of the dermal layer.[19] C_4S is composed of a chain of alternating sugars (N-acetylgalactosamine and glucuronic acid) usually found attached to proteins as part of proteoglycans.[20] Studies have demonstrated the role effectiveness of C_4S in wound healing and tissue regeneration providing structural frameworks for fibroblasts during tissue regeneration.[21]

In this work, the fabrication of electrospun CH-g-PLA nanofibrous scaffolds loaded with AgNP and C_4S, named CH-g-PLA:AgNP:C_4S, was done for the first time *via* electrospinning technique. The effects of process parameters such as solution CH-g-PLA:AgNP:C_4S concentration, viscosity, and ionic conductivity on the morphology of electrospun nanofibers were studied. The electrospun CH-g-PLA:AgNP:C_4S nanofibers scaffolds were studied by scanning electron microscopy (SEM), X-ray diffraction (XRD), and Fourier transform infrared (FTIR). The *in vitro* biocompatibility toward fibroblasts, cell adhesion and proliferation, and antimicrobial properties against *Escherichia coli* (*E. Coli*) and *Staphylococcus aureus* (*S. Aureus*) was characterized.

Experimental

Materials

Chitosan from crab shells (CH) (Sigma-Aldrich, Mw: 1.47×10^5, deacetylation degree: 92.5 mol %), silver nitrate (Fluka, $AgNO_3$, analytical grade), methanol (Sigma-Aldrich, anhydrous, purity: 99.8%), DL-lactic acid (Sigma-Aldrich, purity: 85% w/w), dimethyl formamide (DMF, Sigma-Aldrich), acridine orange (AO) (Sigma-Aldrich), paraformaldeyde (PFA, Sigma-Aldrich), and chondroitin 4-sulfate sodium salt from bovine trachea (Sigma-Aldrich) were used as received. The bacterial species of *E. coli* (LB25922) and *S. aureus* (LB25923) were purchased from Laborclin (Minas Gerais, Brazil).

Methods

Synthesis of CH-g-PLA. CH-g-PLA was synthesized in two steps, the first is the esterification of oligomeric D,L-lactic acid with methanol to produce oligomeric methyl lactate (OMeLAC), and second is the reaction of chitosan with OMeLAC to produce CH-g-PLA. First, 2.0 mols of D,L-lactic acid was autocatalytically polycondensed at 165°C in a 250 ml three-necked double-jacked glass reactor containing 90 g (1.0 mol) of lactic acid, 32 g (1.0 mol) of methanol and 1.0 g of p-toluenesulfonic acid. The glass reactor was attached to a Vigreux fractionating column, and the solution was heated to boiling point in an oil bath. The column was operated under total reflux until the temperature of the vapors at the still head falls at the boiling point of the water–methanol azeotrope (62°C). This azeotrope was then distilled as rapidly as it was formed at 65°C. When the production of methanol has become very slow (8–10 h), the unreacted methanol was distilled, at 65°C under atmospheric pressure. The OMeLAC yield was 80–94%.

The reaction between CH and PLA to obtain CH-g-PLA graft copolymer was synthesized exploring the scope of the ester amidation reaction reported by the literature.[22] CH (50 g) dissolved in acetic acid (3% w/w) was charged in a 250 ml three-necked double-jacked glass reactor connected to a Vigreux fractionating column and vacuum pump. The reactor was purged under nitrogen atmosphere and the temperature was raised to 65°C. Then, 458 parts of OMeLAC are then added dropwise until 1 h with maintenance of the temperature at 55–65°C and total reflux. 1 h after completion of the addition of the OMeLAC, all the methanol has been removed from the reaction mixture by distillation, and titration of the free CH indicates 92% conversion to CH-g-PLA. A highly viscous product having pale brown color was obtained.

In situ electrochemical synthesis of AgNP. The electrochemical synthesis of AgNP dispersed in CH-g-PLA was based on the galvanostatic method (Omnimetra, PG-3901) of an $AgNO_3$ solution, according to a one-step procedure reported in the literature.[23] The electrolysis was performed within a simple two-electrode type electrochemical cell containing an aqueous solution of CH-g-PLA (10 wt%), $AgNO_3$ (1.0 mM), and KNO_3 (0.1 M) at room temperature (25°C) while stirring for 1 h. The volume of the electrolysis cell was 50 mL. A platinum sheet (0.5 cm × 5 cm) was employed as cathode and a platinum rod (0.1 cm × 5 cm) as anode, the

two being 3 cm apart. The cell was maintained into an ultrasonic bath. The solution was purged with N_2 during 30 min. Then, the electrolysis was carried out under ultrasonication at constant current and N_2 atmosphere during 30 min at room temperature (25°C). The current chosen (10 mA) was given by adjusting the applied potential. Silver electrodes were used as cathodes and anodes, respectively. The CH-g-PLA:AgNP were dialyzed using distilled and deionized water in order to remove the $AgNO_3$ residue and then lyophilized.

After AgNP synthesis, an aqueous solution of C_4S (10% w/w) was added to the CH-g-PLA:AgNP and stirred for 1 h to obtain a homogeneous solution. The aqueous solution of CH-g-PLA:AgNP:C_4S was lyophilized to obtain a stable and homogeneous electrospinable colloidal solution.

Electrospinning of CH-g-PLA:AgNP:C_4S. The electrospinning technique was used for the fabrication of electrospun CH-g-PLA:AgNP:C_4S nanofibers. The homogeneous solution of CH-g-PLA:AgNP:C_4S in dimethylformamide (DMF) (10 wt%) was loaded in a 10 mL syringe equipped with a 20 gauge stainless steel needle connected to an electrode of a high voltage power supply (Phywe). The distance from the needle tip to the collector was 10 cm, and 0.5 mL/h of the solution was fed to the needle tip with the applied high voltage of 9 kV between the needle tip and the grounded collector (copper foil). All the experiments were executed at room temperature (20°C). The as-spun CH-g-PLA:AgNP:C_4S fibers were dried in vacuum for 48 h to eliminate the remaining solvent and then stored in the desiccator for further characterizations. Figure 1 illustrates the general procedure to fabricate the electrospun CH-g-PLA:AgNP:C_4S nanofibers.

Characterization methods

Physicochemical characterizations. ^1H and ^{13}C-NMR measurements were carried out on a Varian Unity Plus 500 MHz spectrometer (^1H frequency = 599.81 MHz and ^{13}C frequency = 150.82 MHz) in the proton noise decoupling mode

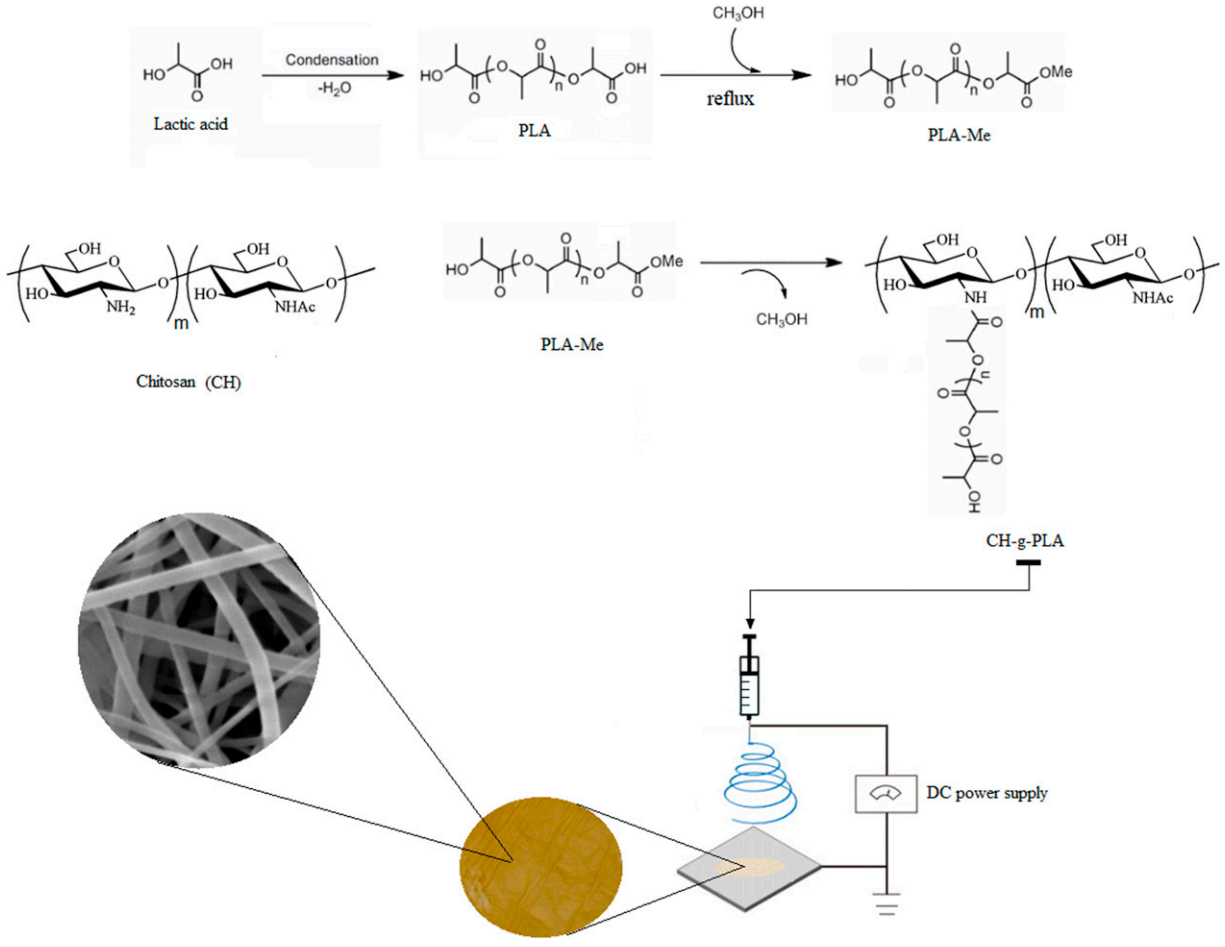

Figure 1. Illustration of the manufacturing process of electrospun CH-g-PLA:AgNP:C_4S nanofibers by electrospinning at room temperature (20°C).

with a standard 5 mm probe. The CH-g-PLA concentration was about 5 wt% in deuterated water (D_2O). The chemical shift was referenced to signals of the solvent and tetramethylsilane (TMS). To reduce the interference of the solvent signal (D_2O) with the sample peaks, the experiment was conducted at a temperature of 70°C.

FTIR spectra of the CH-g-PLA were recorded on a Shimadzu IRTracer 100 spectrometer (Shimadzu) in the spectral region of 650 and 4000 cm^{-1} with a resolution of 1 cm^{-1}, setting 50 scans for a single analysis and using PIKE MIRacle Attenuated Total Reflection (ATR) accessory.

UV-Vis spectroscopy was performed to monitor the formation of AgNP by the presence of characteristic plasmon bands. The analyses were carried out using UV-Vis Varian CARY 50 equipment in scan mode, in the 200–800 nm range with quartz cuvettes.

The X-ray diffraction (XRD) pattern of the CH-g-PLA:AgNP:C_4S was recorded by employing a Ultima IV (Rigaku) X-ray diffractometer with scans of 2°/min from 5 to 90 Å, copper Kα radiation (λ = 1.5418 Å), 30 mA current, 40 kV voltage, step of 0.0202°, and 2θ/θ scanning mode to observe peaks that were possibly indicative of crystallinity.

Sessile drop method was used to evaluate surface wettability of the electrospun CH-g-PLA:AgNP:C_4S using a Krüss Easy Drop FM40 equipped with a CCD camera. Distilled and deionized water was used as a testing liquid at 20°C and 60% relative humidity. Droplet volume of 5 µL was set for each experiment, and 10 separated drops were placed to the each sample surface for 20 s to obtain the water contact angle (WCA).

Morphological studies of electrospun CH-g-PLA:AgNP:C_4S nanofibers were carried out using a Phillips XL30 FEGSEM (JSM-6701F) scanning electron microscope (SEM, Phillips), operating with vacuum conditions of 7×10^{-6} Torr at an accelerating voltage of 10 kV. Samples were gold metallized by an Auto Sputter Coater. Images were taken with 5000 SEM micrograph magnifications. The diameters of 100 randomly selected electrospun CH-g-PLA:AgNP:C_4S nanofibers were measured using image analysis software (ImageJ, National Institute of Health, Bethesda, MD, United States). For the determination of the mean diameter, micrographs were analyzed with magnification of × 5000 considering three different fields of different samples.

The effect of conductivity and viscosity on the electrospinning process has been investigated. Conductivity measurements of CH-g-PLA:AgNP:C_4S solutions in dimethylformamide (DMF) were carried out using a Metler Toledo S230 pH/mV/conductivity meter. The viscosity of the different solutions was determined using a rotational Brookfield IKA Rotavisc viscometer equipped with a small sample adapter (SSA).

The silver and C_4S release from electrospun CH-g-PLA:AgNP:C_4S nanofibers was studied under static conditions. The samples were immersed in a phosphate buffer solution (PBS, pH 7.4). During the entire experiment, the bottles containing the PBS and samples were stored at 37°C, to simulate natural physiological conditions. The PBS solution was changed periodically, that is, every 24 h for 7 days, and then roughly every 5–7 days, for a total of 28 days. The concentration of silver released from the electrospun CH-g-PLA:AgNP:C_4S nanofibers into the PBS was measured with an UV-Vis absorption spectrophotometer (Varian Cary 50) using the surface plasmon resonance (SPR) band of silver at λ_{max} of 411 nm.[24]

The amount of C_4S released from electrospun CH-g-PLA:AgNP:C_4S nanofibers was determined by methylene blue (MB) assay.[25] The assay is based on the observation that the absorbance of MB at 664 nm decreases when complexation to C_4S occurs. The decrease in the absorption at 664 nm is proportional to the concentration of C_4S in the solution, providing a basis for the quantitative determination of chondroitin sulfate by methylene blue. Calibration curves were carried out by reading the absorbance at 664 nm by a series of MB solutions containing a fixed amount of MB and increasing amount of the C_4S.[25]

In Vitro *Antibacterial activity of electrospun CH-g-PLA:AgNP:C_4S nanofibers.* To investigate the antibacterial activity of CH-g-PLA:AgNP:C_4S, *E. coli* and *S. aureus* were used in this study. Antibacterial activities were investigated by agar disc diffusion assay and modified liquid growth inhibition assay as described previously.[26] The electrospun CH-g-PLA:AgNP:C_4S nanofibers were punched to make film discs (8 mm in diameter) and sterilized in the laminar air flow chamber by exposure to a UV-C lamp (30 min, distance from the lamp 60 cm). A soft-top agar (1.0 wt %, 20 ml) was melted, cooled to 55°C and inoculated with overnight (18 h) bacteria cultures (200 µL), then gently stirred, and poured over previously solidified nutrient agar base in sterile Petri dishes. Number of bacteria in the nutrient soft-top agar layer was set to be 1.5×10^8 CFU. mL^{-1}. After solidification of soft-top agar, CH-g-PLA:AgNP:C_4S disc samples were placed on its surface. The widths of inhibition zones were measured after 24 h incubation at 37°C. Each assay was carried out in triplicates.

Cytotoxicity assay. Electrospun CH-g-PLA:AgNP:C_4S nanofibers were tested for cytotoxicity against tissue-specific cell culture Mouse L929 fibroblast cells.[27] Before testing, electrospun CH-g-PLA:AgNP:C_4S nanofibers was sterilized by exposure to ultraviolet light for 30 min for each surface. Only viable cells (viability >90%) were harvested and counted by 0.1% trypan blue exclusion. L929 growth inhibition was evaluated by MTT assay, based on

the cleavage of the tetrazolium salt MTT (3-(4,5-dimethylthiazol-2-yl)-2,5-diphenyl tetrazolium bromide) to formazan by mitochondrial dehydrogenases in viable cells. The electrospun CH-g-PLA:AgNP:C_4S samples were then incubated in 1 mL of DMEM at 37°C for 24 h. After that, the CH-g-PLA:AgNP:C_4S samples were removed and the extracts were obtained and further diluted to get extraction medium samples. Viable L929 fibroblast cells were plated in 100 µL of complete medium per well (96-well microtiter plates), incubated at 37°C for 24 h. After incubation for another 24 h, the culture medium was removed and replaced with the extraction medium and incubated for 24 h. Then, about 100 µL of MTT solution was added to each well. After 24 h incubation at 37°C, 200 µL of dimethyl sulfoxide (DMSO) was added to dissolve the formazan crystals. The optical density of the formazan solution was detected by an ELISA reader (Multiscan Dynatec MR5000) at 490 nm. For reference purposes, cells were seeded to medium containing 0.50% phenol (positive control) and a fresh culture medium (negative control) under the same seeding conditions, respectively. The inhibition of growth was expressed as percent of control.

After the viability assay, the CH-g-PLA:AgNP:C_4S samples were washed with phosphate-buffered saline solution (PBS) pH 7.4 and fixed with PFA 4% (w/v) for 30 min at 4°C. The PFA was then removed, and the CH-g-PLA:AgNP:C_4S samples were washed again with PBS. Cytoskeleton cells were stained with acridine orange (AO, Sigma-Aldrich) 1 mM for 5 min for further imaging using a fluorescence microscope Carl Zeiss fluorescence microscope, model Axioskop 40 at magnification of × 200.

Statistical analysis

All experiments were carried out in triplicate, and average values with standard deviation were reported. Data were analyzed using R version 4.0.5. One-way analysis of variance (ANOVA) was used for the statistical analysis. Values of $p < .05$ were considered to be a statistically significant finding.

Results and discussion

Structural analysis of CH-g-PLA

Figure 2 shows the ^{1}H-NMR spectrum of electrospun CH-g-PLA nanofibers in D_2O at 70°C. The resonances to protons of N-acetylglucosamine (GlcN) units are observed at 4.2–4.4 ppm (H-1), 3.6–4.0 ppm (H-3, H-4, H-5, and H-6), and 3.1 ppm (H-2*) are characteristics of chitosan.[28] The signals located at 1.3 ppm (H-a)-1.42 ppm (H-a*) are assigned to protons of methyl (CH_3) in PLA main chain and adjacent to end hydroxyl groups of the polyester, respectively. The proton signal at 2.1 ppm (H-2) (Figure 2) revealed the amide linkage, which further confirmed the successful grafting of CH by PLA.[29] PLA branches were inserted in the concentration around 33.4% (mol PLA/100 mol glucose ring in relation to the nongrafted CH) as pointed by the ratio of the integral peaks for H-2 and H-2* of GlycN ring (Figure 2). The chemical strategy (Figure 2) was based in the esterification reaction of the carboxyl end groups of the PLA with the amino groups of CH. The integral ratio of H-2* to the sum of H-2* and H-2 was 0.3/(0.3 + 0.6) and confirms that substitution degree of PLA onto CH was around 33.4%.

CH and the CH-*g*-PLA were characterized by ATR-FTIR spectroscopy and their spectra are shown in Figure 3. The spectrum of CH showed the typical absorption bands at 3400 cm^{-1} (-OH and -NH stretch), a weak band at 2878 cm^{-1} (-CH stretch), two middle strong bands at 1640 and 1570 cm^{-1} (amide I and II, respectively), 1037 and 1890 cm^{-1} (saccharide structure), and 1400 and 1250 cm^{-1} (-OH and -CH bend). These absorption bands are observed after PLA graft polymerization which indicates that the polysaccharide backboned is conserved after amidation reaction with the polyester. The most important evidence of the obtaining of CH-g-PLA copolymer was the absorption bands observed at 1718 and 1121 cm^{-1} attributed to the vibration stretch of C=O of carbonyl ester band and C-O-C of the PLA grafts (Figure 3), respectively. These bands are absent in the spectrum of CH. Moreover, the ATR-FTIR spectra of CH-g-PLA show a pronouncedly decrease in the intensity of the absorption bands at 3400 cm^{-1} attributed to the NH stretch vibrations (Figure 3). This suggests that the grafting of PLA occurs through the rupture of N-H bonds of CH, which are the most labile. The peaks at about 1037 and 1076 cm^{-1}, which belong to the C-O-C stretching and the C–OH stretching of PLA, are visible in CH-g-PLA spectra (Figure 3) and are in good agreement with the literature.[9]

UV-Vis spectroscopy analysis was used to observe AgNP produced by electrochemical reduction, and the results are shown in Figure 4. The results of UV-Vis spectroscopy of the solution of AgNP shows that there is only a single optical absorption peak around 435 nm (Figure 4), due to the collective oscillations of the surface plasmons, that is, collective oscillations of the conduction band electrons of the constituent atoms of the AgNPs, induced by incident UV-Vis light. Moreover, the single peak (Figure 4) suggests that the AgNPs produced have size around 30 nm and geometry close to spherical, causing there to be only one mode of oscillation of the surface plasmons.[30]

The typical XRD pattern of electrospun CH-g-PLA:AgNP:C_4S nanofibers is depicted in Figure 5. The Bragg reflections at 38.5 and 44.3° are related to the (111) and (200) Miller indices (JCPDS 04-0783) and confirms the presence of AgNP with a cubic crystalline structure with a centered face (fcc) inside the electrospun CH-g-PLA:AgNP:

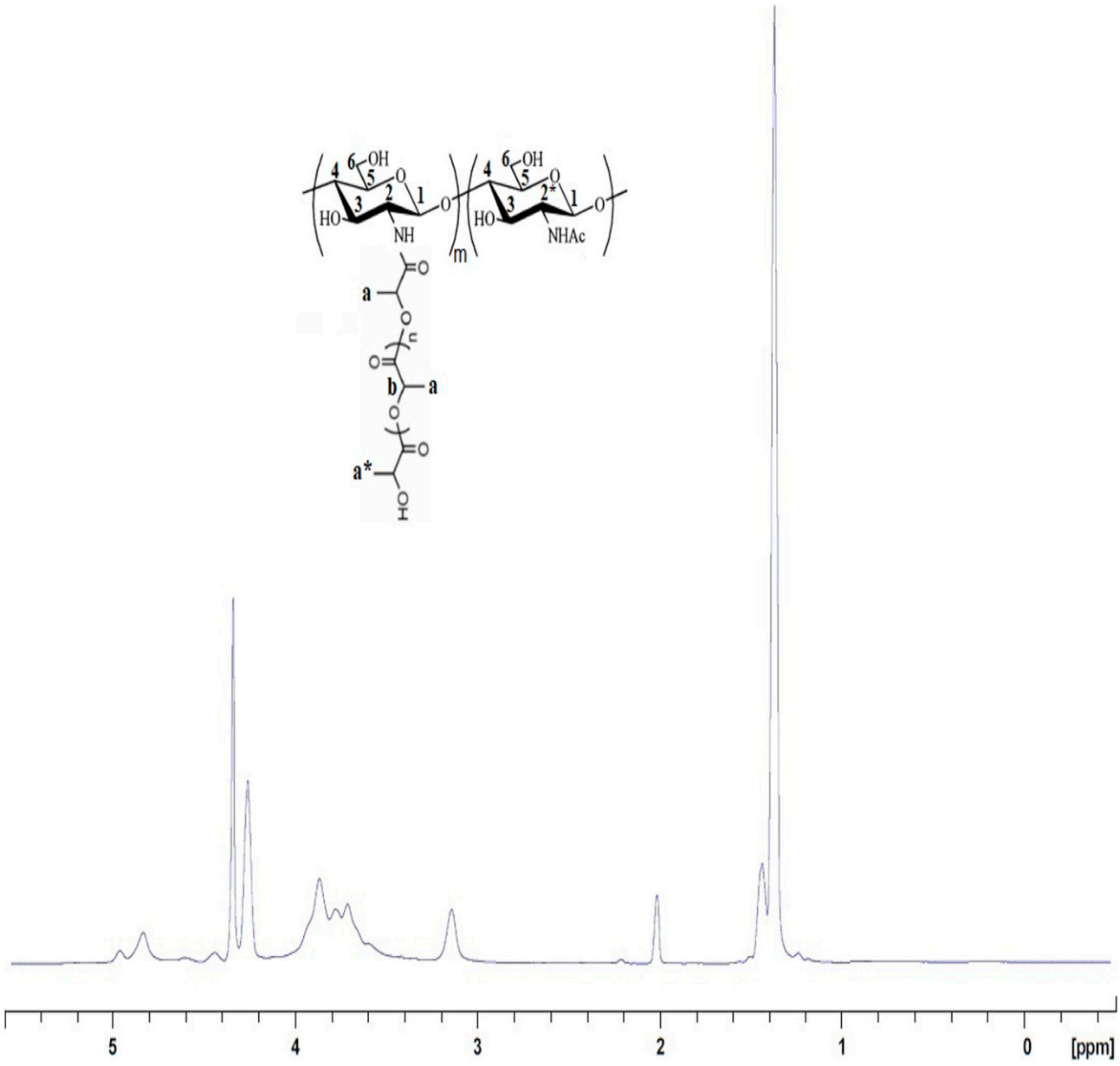

Figure 2. ^{1}H-NMR (nuclear magnetic resonance) spectra of CH-g-PLA measured at 70°C to reduce the interference of the solvent signal (D_2O).

C_4S nanofibers.[31] The others peaks at 2θ = 17.5, 28.5 and 32° are related to CH-g-PLA:C_4S composition. The full width at half maximum (FWHM) value of the (111) crystalografic plane was used to calculate the size of the AgNP using Scherrer's equation.[32] The average crystallite size of the AgNPs from electrospun CH-g-PLA:AgNP:C_4S nanofibers was found to be around 28 nm and appears to be consistent with the results found in the UV-Vis technique (Figure 4).

The SEM images of the electrospun CH-g-PLA:AgNP:C_4S nanofibers are depicted in Figure 6(a). SEM micrographs (6a) shows smooth and continuous electrospun CH-g-PLA:AgNP:C_4S nanofibers with good structural integrity. A normal distribution was observed throughout the data with a mean of 340 ± 18 nm as the most frequently observed (Figure 6(b)). The fibers formed from CH-g-PLA:AgNP:C_4S in DMF (10 wt%) are smooth and continuous (Figure 6(a)). However, increasing the concentration of CH-g-PLA:AgNP:C_4S beyond 10 wt.% leads to the decrease in the structural integrity by the formation of defective nanofibers such as balloons (Figures 6(c) and (d)). This result suggests that the CH-g-PLA:AgNP:C_4S concentration has a

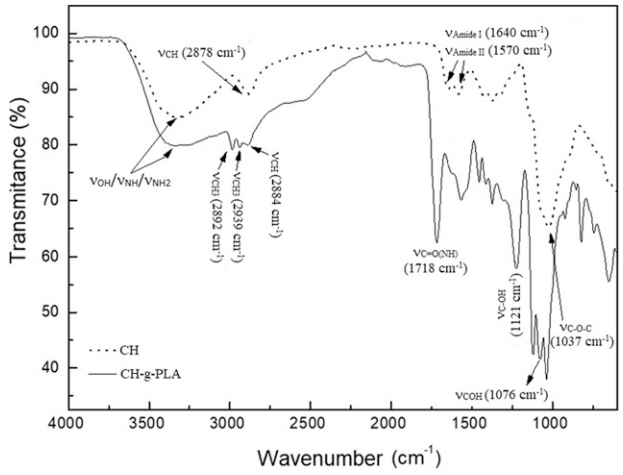

Figure 3. ATR-FTIR spectra of CH, and CH-g-PLA measured at room temperature (25°C), with ν representing the stretching vibration of chemical bonds of CH and CH-g-PLA, respectively.

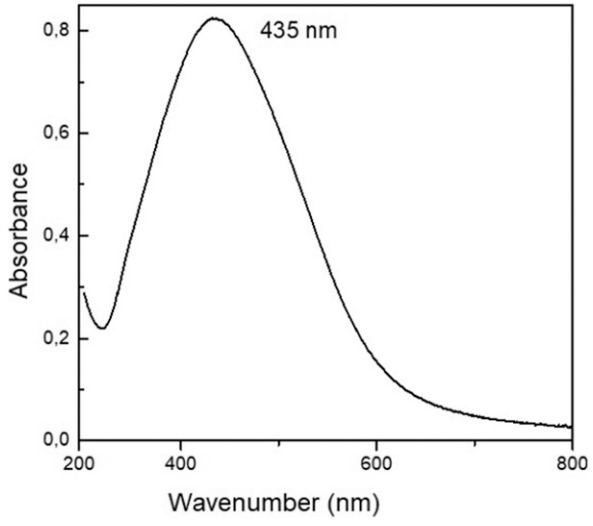

Figure 4. UV-Vis spectra of AgNPs incorporated on electrospun CH-g-PLA nanofibers measured at room temperature (25°C).

direct impact on the whipping and stretching of the polymer jet during electrospinning process. A decrease in whipping occurs with increasing CH-g-PLA:AgNP:C_4S concentration due to the physical weight of graft copolymer and the interaction of the CH-g-PLA:AgNP:C_4S with DMF within the jet. This explains the loss of the structural integrity of the electrospun CH-g-PLA:AgNP:C_4S nanofibers with the formation of defective nanofibers (Figures 6(c) and (d)).[33]

The morphology of the electrospun CH-g-PLA:AgNP:C_4S nanofibers depends on various processing parameters conditions. In order to gain control over the properties of the electrospun CH-g-PLA:AgNP:C_4S nanofibers such as

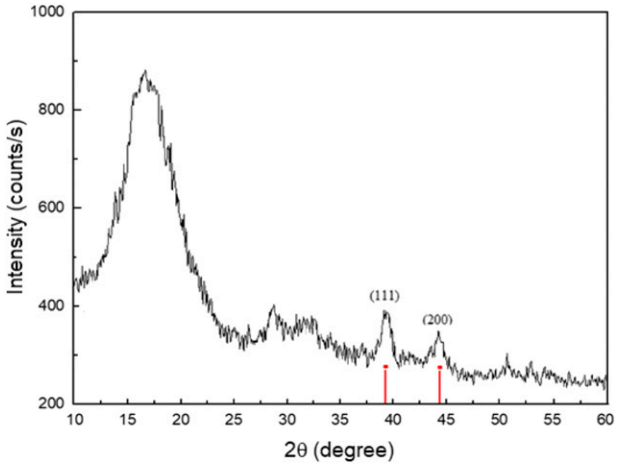

Figure 5. X-ray diffraction pattern of electrospun CH-g-PLA:AgNP:C_4S nanofibers measured at room temperature (25°C).

diameter, porosity, and morphology, the viscosity and the electrical conductivity were measured as function of the solution CH-g-PLA:AgNP:C_4S concentration in DMF. Figure 7 shows that the viscosity increases steadily with polymer concentration going from 15 mPa.s at 2 wt.% to 362 mPa.s at 10 wt.% and 3462 mPa.s at 20 wt.%. The electric conductivity of polymer solutions was between 25 $\mu S.cm^{-1}$ (2 wt. %), 71 $\mu S.cm^{-1}$ (10 wt. %), and 32 $\mu S/cm^{-1}$ (20 wt.%) (Figure 7). The conductivity first increases going from 2 to 10 wt.% to then decrease with increasing CH-g-PLA:AgNP:C_4S concentration due to the high dielectric constant (36.71 at 25°C) and dipole moment (3.24 Debye) of DMF.[34] These results indicate that a spinning CH-g-PLA:AgNP:C_4S solution with a ionic conductivity of 29.8 $\mu S.cm^{-1}$, viscosity of 2959 mPa.s, and values of concentration around 10 wt.% is considered to be suitable for CH-g-PLA:AgNP:C_4S electrospinning.

The biological response to electrospun CH-g-PLA:AgNP:C_4S nanofibers could be influenced by the hydrophilicity and porosity, considered as important surface properties that affecting cell adhesion and proliferation of fibroblast cells.[35] The contact angle measurements were made to enable us to understand the wettability of the electrospun CH-g-PLA:AgNP:C_4S nanofibers, and the results are shown in Figure 8. The average contact angle of the CH-g-PLA:AgNP (35,3 ± 3.4°) and CH-g-PLA:AgNP:C_4S (12.8 ± 2.7°) reveals the hydrophilic nature of the electrospun nanofibers (Figure 8) as well as the role of C_4S in bestowing hydrophilicity to the electrospun CH-g-PLA:AgNP:C_4S nanofibrous material. The improvement in hydrophilicity with the addition of C_4S is expected to lead to higher fibroblast affinity of the electrospun CH-g-PLA:AgNP:C_4S nanofibers compared to CH-g-PLA:AgNP.[36]

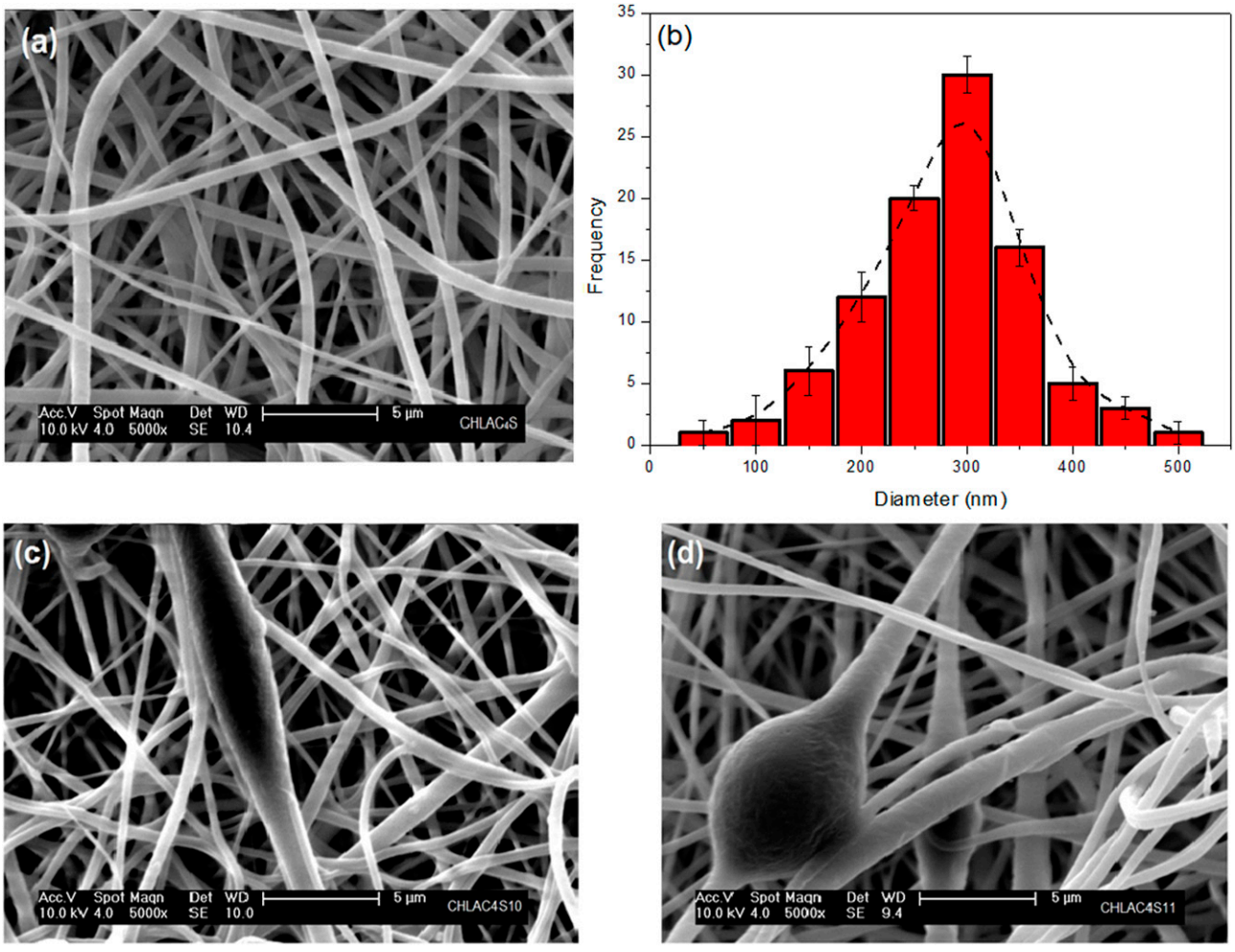

Figure 6. Scanning electron microscope (SEM) micrographs of electrospun CH-g-PLA:AgNP:C_4S nanofibers at 10 wt% (a) and 13 wt% (c,d) produced using dimethyl formamide (DMF) as solvent. The histogram of distribution is shown in (b).

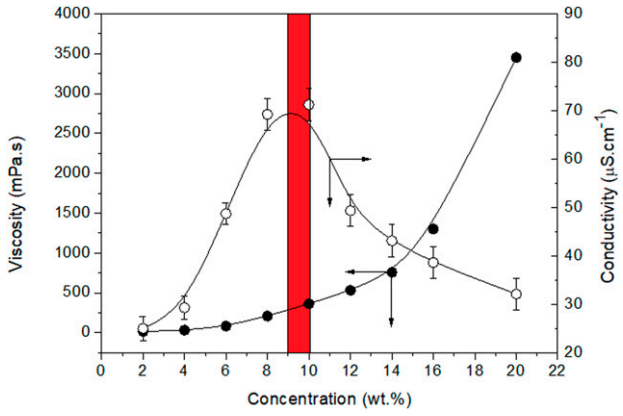

Figure 7. Solution viscosity and electrical conductivity as function of the CH-g-PLA:AgNP:C_4S concentration measured at room temperature (25°C). Solvent: DMF. The red shaded area indicates the most suitable region for the electrospinning of CH-g-PLA:AgNP:C_4S solution.

The electrospun CH-g-PLA:AgNP:C_4S porosity (p) was determined by gravimetric method in according to equation (1) [37]

$$P = \left[1 - \frac{m}{A.h.\rho_o}\right].100 \quad (1)$$

where, ρ, m, A, h, and ρ_o are the apparent density, mass, area, thickness, and the bulk density of the electrospun CH-g-PLA:AgNP:C_4S nanofibers, respectively.

In this work, electrospun CH-g-PLA:AgNP:C_4S nanofibers with porosity of 89 ± 3.08% and an average pore area of 0.27 μm^2 were obtained. The high values of porosity and average pore area should be suitable for fibrolast adhesion and proliferation onto electrospun CH-g-PLA:AgNP:C_4S nanofibers because the extracellular matrix is composed of nanofibrillar components.[38]

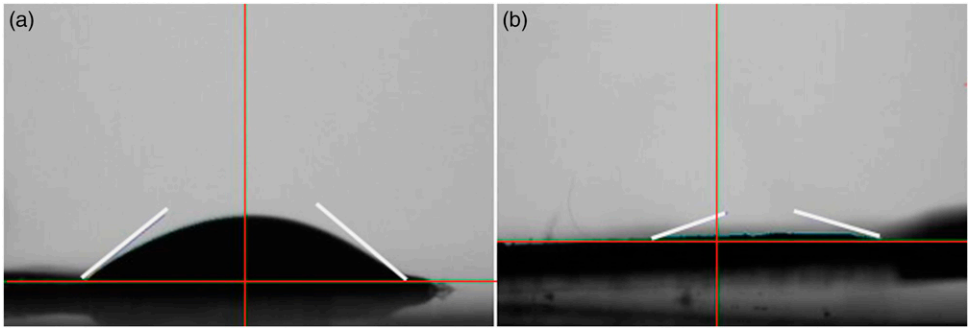

Figure 8. Contact angle of CH-g-PLA:AgNP (a) and CH-g-PLA:AgNP:C_4S (b) electrospun materials at room temperature (25°C).

In vitro *Ag^+ and C_4S release*

The silver ions (Ag^+) release profiles of electrospun CH-g-PLA:AgNP:C_4S nanofibers which are shown in Figure 9. It is seen that the Ag^+ ions from electrospun CH-g-PLA:AgNP:C_4S nanofibers release rate are relatively high in the first few days and then level off over time. The cumulative releases over 10 days for the electrospun CH-g-PLA:AgNP:C_4S nanofibers were approximately 40 part per million (ppm), and a steady release rate of Ag^+ ions at around 1 ppm per day was attained. It was reported that a steady and prolonged Ag^+ release rate at a concentration level as low as 0.1 part per billion (ppb) is necessary to provide effective antibacterial properties.[39] Then, the results indicate that electrospun CH-g-PLA:AgNP:C_4S nanofibers can release sufficient amounts of Ag^+ to exhibit sustained antibacterial activity.

Recent studies indicates that C_4S is able to stimulate the wound healing process in a complex mechanism regulated by signaling molecules produced by a wide range of cells present in the extracellular matrix (ECM).[40] C_4S is an important group of ECM proteins that plays a significant role in each stage of the wound healing process.[41] Besides the characteristics discussed above, the local release of C_4S can improve the final properties of electrospun CH-g-PLA:AgNP:C_4S nanofibers stimulating the wound repair.

Figure 9 shows the fraction of C_4S released *in vitro* from the electrospun CH-g-PLA:AgNP:C_4S nanofibers as a function of time. The release profile (Figure 9) showed that the fraction of C_4S released in vitro increased up to 12 days and then the equilibrium is achieved. Release data obtained from the electrospun CH-g-PLA:AgNP:C_4S nanofibers in physiological conditions (phosphate buffer, 50 mM, pH 7.4) indicated a higher retention of C_4S (around 58% release in 10 days). The higher retention of C_4S in electrospun CH-g-PLA:AgNP:C_4S nanofibers suggests a strong complexation type polycation-polyanion interactions between non-grafted amino groups of CH and sulfate groups of C_4S.[42] Then, the complexes formed are very strong and could favor the entrapment of C_4S molecules within electrospun CH-g-PLA:AgNP:C_4S nanofibers.

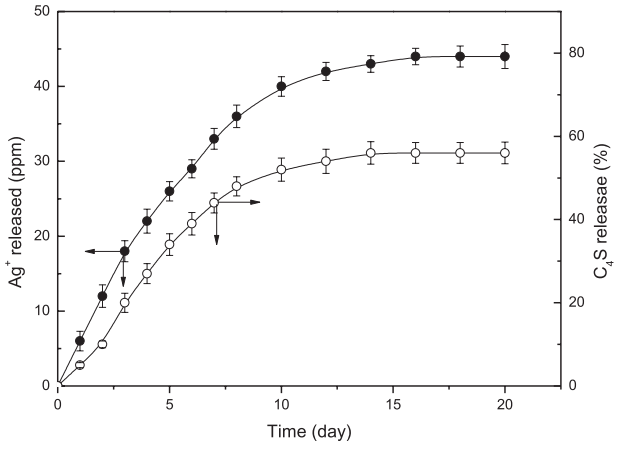

Figure 9. *In vitro* release profiles of Ag^+ ions (•) and C_4S (○) from electrospun CH-g-PLA:AgNP:C_4S nanofibers as a function of time in phosphate buffer solution (PBS, 50 mM, pH 7.4) and 37°C (mean values ± SD; n = 3).

In vitro *biological characterization*

Antimicrobial properties. It is well known that bacteria are present on all skin surfaces. However, when the primary defense of the intact skin disappears, the bacteria start to reside on the wound surface. The infection arises due to lack of oxygen, nutrition, antibodies, or the presence of biofilms in the injured tissue.[43] Bacterial wound infection is probably the most common cause of delayed healing process. The most prevalent microorganisms founded in infected wounds are *S. aureus* and *E. Coli*.[44] For these reasons, antimicrobial properties of electrospun CH-g-PLA:AgNP:C_4S nanofibers against *E. coli* and *S. aureus* were assessed.

Figure 10 reports the results of antimicrobial properties of electrospun CH-g-PLA:AgNP:C_4S nanofibers evaluated against *S. aureus* and *E. coli*, Gram (+) and Gram (−) microorganisms, respectively. Chlorhexidine

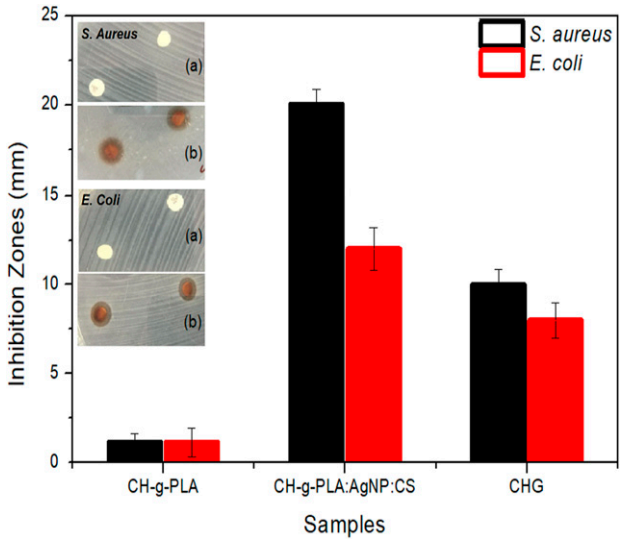

Figure 10. Antibacterial activity of electrospun CH-g-PLA:AgNP:C_4S nanofibers against S. aureus and E. coli through agar diffusion discs assays on agar plates (inserted image). The chlorhexidine gluconate (CHG) 0.2% was used as a positive control and CH-g-PLA as a negative control. The error bars indicate the mean ± SD (n = 3). The microbiological test micrograph is represented by the inserted image where (a) represents the CH-g-PLA and (b) represents the electrospun CH-g-PLA:AgNP:C_4S nanofibers.

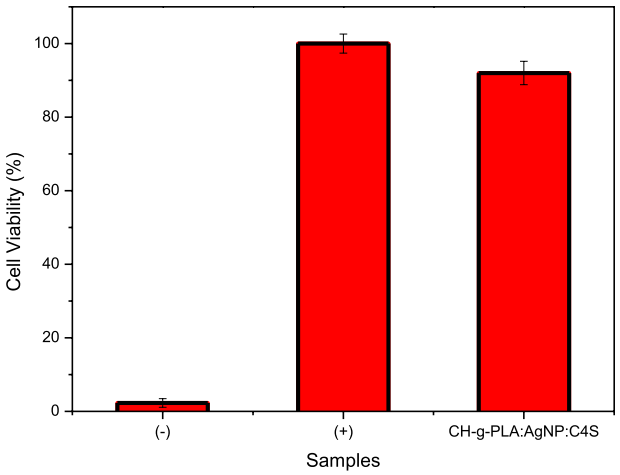

Figure 11. Cell proliferation of L-929 cells evaluated by MTT assay after 24 h of incubation with 0.50% phenol as negative control (−), fresh culture medium as positive control (+) and CH-g-PLA:AgNP:C_4S.

gluconate (CHG) 0.2% was used as a positive control because this is a germicidal agent commonly used in healthcare services, while CH-g-PLA was used as control negative as there is no antibacterial effect found. No zone inhibition was observed in the negative controls, which contained the culture supernatant or sterile nutrient broth and CH-g-PLA (Figure 10). Disc diffusion assay showed that electrospun CH-g-PLA:AgNP:C_4S nanofibers can inhibit significantly the growth of both, *S. aureus* and *E. coli* (Figure 10). The tests confirm that the antimicrobial activity of the electrospun CH-g-PLA:AgNP:C_4S nanofibers was superior to CHG for both, *S. aureus* and *E. coli* microorganisms (Figure 10). The result found is in agreement with the scientific literature recently reported, which tested the AgNPs against *S. aureus* and *E. coli*. The Ag^+ ions binds to the teichoic acids (TAs) founded within the cell wall of the most Gram-positive bacteria altering their permeability resulting in weakening of the cell wall and the formation of reactive oxygen species (ROS).[45] The ROS seems to be the principal mechanism responsible by the quickly inhibition of the growth and reproduction of bacterial cells.[46] The inhibition growth of *S. aureus* and *E. coli* observed in the current study indicates the potential use of electrospun CH-g-PLA:AgNP:C_4S nanofibers as an antimicrobial scaffold for tissue engineering. The electrospun CH-g-PLA:AgNP:C_4S nanofibers, which are in contact with skin and wound tissue, interact with moisture resulting in the release of Ag^+ ions promoting the antimicrobial effect. Moreover, it is also important to determine the cytotoxicity of electrospun CH-g-PLA:AgNP:C_4S nanofibers when considering its clinical application.

Cytotoxicity properties. Figure 11 shows the results of the cytotoxicity assay of electrospun CH-g-PLA:AgNP:C_4S nanofibers using L-929 fibroblasts as the mammalian cell model. As it can be seen, the electrospun CH-g-PLA:AgNP:C_4S nanofibers do not have the negative effect on cell viability. The non-cytotoxicity of the electrospun CH-g-PLA:AgNP:C_4S nanofibers can most likely be attributed to an ideal hydrophobic–hydrophilic balance established by the presence of the grafted PLA and C_4S chains, respectively.[47]

Fluorescence analysis of adhered cells onto electrospun nanofibers. Figure 12 shows the fluorescence microscopy of fibroblast cells adhered onto CH-g-PLA:AgNP:C_4S and CH-g-PLA:AgNP scaffolds to study the influence of the C_4S on proliferation of the fibroblast cells onto electrospun nanofibers. The adhered fibroblasts cells onto CH-g-PLA:AgNP:C_4S and CH-g-PLA:AgNP were stained with AO. Both types of scaffolds promote adhesion and proliferation of fibroblast cells (Figure 12). However, it is evidenced on fluorescence optical images (Figure 12) that electrospun CH-g-PLA:AgNP:C_4S nanofibers exhibit more proliferation of L929 mouse fibroblast cells relatively to electrospun CH-g-PLA:AgNP nanofibers after 24 h, as expected. It is well known that C_4S as constituents of native tissues is

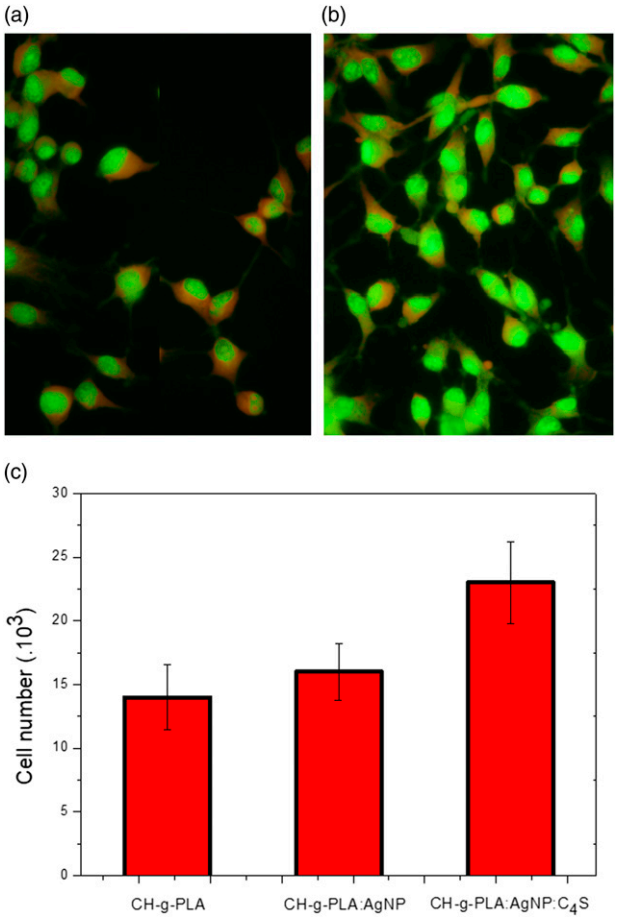

Figure 12. Fluorescence microscopy analysis of fibroblast L-929 cells adhered to the CH-g-PLA:AgNP (a) and CH-g-PLA:AgNP:C_4S (b) after 24 h of incubation. Magnification: × 200. The number of adhered cells for different electrospun substrates seeded with 1.5 × 10^5 cells are shown in (c). Data are reported as means ± SD.

widely utilized to produce scaffolds serving as an active analog of native extracellular matrix (ECM).[48]

Conclusion

Chitosan (CH)-grafted poly(lactic acid) (PLA) was successfully synthesized via amidation chemical route. Electrospun nanofibers were prepared from mixed solutions of partially chondroitin sulfate, silver nanoparticles (AgNPs), and CH-g-PLA. AgNPs around 30 nm were *in situ* synthesized by electrochemical reduction of $AgNO_3$ in CH-g-PLA:C_4S aqueous solution. SEM results showed that highly porous electrospun CH-g-PLA:AgNP:C_4S nanofibers with diameter of 340 ± 18 nm, porosity of 89 ± 3.08%, and an average pore area of 0.27 μm^2 were obtained. The addition of C_4S to CH-g-PLA nanofibers would increase the hydrophilicity of electrospun nanofibers as evidenced by contact angle measurements. Furthermore, the electrospun CH-g-PLA:AgNP:C_4S nanofibers exhibited antibacterial activity against S. Aureus and *E. coli*. Based on the MTT assays, CH-g-PLA:AgNP:C_4S nanofibers exhibited no cytotoxicity to the L929 cells fibroblast cells. Fluorescent microscopy evidenced that adhesion and colonization of electrospun PLA-g-CH:AgNP:C_4S nanofibers by fibroblast cells was favored by C_4S. Therefore, the electrospun PLA-g-CH:AgNP:C_4S nanofibers exhibited both antibacterial activity and non-cytotoxicity to the mammalian cells, making them potential candidates for biomedical applications, which will be explored in the near future.

Acknowledgments

Authors thank gratefully the financial support received from National Council for Scientific and Technological Development (CNPq, Ref No. 307609/2018-9) and the Improvement of Higher Education Personnel (Capes) for carrying out this research work.

Declaration of conflicting interests

The authors declare that there is no conflict of interests regarding the publication of this work.

Funding

The author(s) disclosed receipt of the following financial support for the research, authorship, and/or publication of this article: This study is supported by Conselho Nacional de Desenvolvimento Científico e Tecnológico (307609/2018-9).

ORCID iDs

Alexandre F Júnior https://orcid.org/0000-0003-4810-555X
Alvaro A Alencar de Queiroz https://orcid.org/0000-0002-1769-7022

References

1. Jiménez-Gómez CP and Cecilia JA. Chitosan: A natural biopolymer with a wide and varied range of applications. *Molecules* 2020; 25: 1–43.
2. Wang W, Meng Q, Li Q, et al. Chitosan derivatives and their application in biomedicine. *Int J Mol Sci* 2020; 21: 1–26.
3. Nasrabadi M, Beyramabadi SA and Morsali A. Surface functionalization of chitosan with 5-nitroisatin. *Int J Biol Macromolecules* 2020; 147: 534–546.
4. Azmy EAM, Hashem HE, Mohamed EA, et al. Synthesis, characterization, swelling and antimicrobial efficacies of chemically modified chitosan biopolymer. *J Mol Liquids* 2019; 284: 748–754.
5. Li J, Kong M, Cheng XJ, et al. Preparation of biocompatible chitosan grafted poly (lactic acid) nanoparticles. *Int J Biol Macromolecules* 2012; 51: 221–227.
6. Kaliva M, Georgopoulou A, Dragatogiannis DA, et al. Biodegradable chitosan-graft-poly (l-lactide) copolymers for bone tissue engineering. *Polymers* 2020; 12: 1–19.

7. Zhan S, Liu N, Wang W, et al. Preparation and characterization of chitosan-graft-poly (L-lactic acid) microparticles. *Polym Eng Sci* 2016; 56: 1432–1436.
8. Suyatma NE, Copinet A, Legin-Copinet E, et al. Different pla grafting techniques on chitosan. *J Polym Environ* 2011; 19: 166–171.
9. Di Martino A and Sedlarik V. Amphiphilic chitosan-grafted-functionalized polylactic acid based nanoparticles as a delivery system for doxorubicin and temozolomide co-therapy. *Int J Pharmaceutics* 2014; 474: 134–145.
10. Su F, Wang J, Zhu S, et al. Synthesis and characterization of novel carboxymethyl chitosan grafted polylactide hydrogels for controlled drug delivery. *Polym Adv Tech* 2015; 26: 924–931.
11. Di Martino A, Kucharczyk P, Zednik J, et al. Chitosan grafted low molecular weight polylactic acid for protein encapsulation and burst effect reduction. *Int J Pharmaceutics* 2015; 496: 912–921.
12. Bhattarai N, Ramay HR, Chou SH, et al. Chitosan and lactic acid-grafted chitosan nanoparticles as carriers for prolonged drug delivery. *Int J Nanomedicine* 2006; 1: 181–187.
13. Hardiansyah A, Tanadi H, Yang MC, et al. Electrospinning and antibacterial activity of chitosan-blended poly (lactic acid) nanofibers. *J Polym Res* 2015; 22: 1–10.
14. Li F, Liu C, Gao Q, et al. Electrospinning of chitosan/poly (lactic acid) nanofibers: the favorable effect of nonionic surfactant. *J Appl Polym Sci* 2014; 131: 1–8.
15. Thomas MS, Pillai PKS, Faria M, et al. Electrospun polylactic acid-chitosan composite: A bio-based alternative for inorganic composites for advanced application. *J Mater Sci Mater Med* 2018; 29: 137–212.
16. Tighzert W, Habi A, Ajji A, et al. Fabrication and characterization of nanofibers based on poly (lactic acid)/chitosan blends by electrospinning and their functionalization with phospholipase A1. *Fibers Polym* 2017; 18: 514–524.
17. Paladini F and Pollini M. Antimicrobial silver nanoparticles for wound healing application: Progress and future trends. *Materials* 2019; 12: 1–16.
18. Xu L, Wang YY, Huang J, et al. Silver nanoparticles: Synthesis, medical applications and biosafety. *Theranostics* 2020; 10: 8996–9031.
19. Smith MM and Melrose J. Proteoglycans in normal and healing skin. *Adv Wound Care* 2015; 4: 152–173.
20. Lamari FN and Karamanos NK. Structure of chondroitin sulfate. *Adv Pharmacol* 2006; 53: 33–48.
21. Sikka MP and Midha VK. The role of biopolymers and biodegradable polymeric dressings in managing chronic wounds. In: Rajedran S (ed) *Advanced Textiles for Wound Care*. 2nd ed. Cambridge, UK: Elsevier Science Technology, 2019, pp. 463–488
22. Gnanaprakasam B and Milstein D. Synthesis of amides from esters and amines withlLiberation of H2 under neutral conditions. *J Am Chem Soc* 2011; 133: 1682–1685.
23. Starowicz M, Stypuła B and Banaś J. Electrochemical synthesis of silver nanoparticles. *Electrochemistry Commun* 2006; 8: 227–230.
24. Bhui DK, Bar H, Sarkar P, et al. Synthesis and UV-vis spectroscopic study of silver nanoparticles in aqueous SDS solution. *J Mol Liquids* 2009; 145: 33–37.
25. Zhou SG, Jiao QC, Chen L, et al. Binding interaction between chondroitin sulfate and methylene blue by spectrophotometry. *Spectrosc Lett* 2002; 35: 21–29.
26. Regiel A, Irusta S, Kyzioł A, et al. Preparation and characterization of chitosan-silver nanocomposite films and their antibacterial activity againstStaphylococcus aureus. *Nanotechnology* 2013; 24: 015101.
27. Ozdemir KG, Yılmaz H and Yılmaz S. *In vitro* evaluation of cytotoxicity of soft lining materials on L929 cells by MTT assay. *J Biomed Mater Res Appl Biomater* 2009; 90: 82–86.
28. Lavertu M, Xia Z, Serreqi AN, et al. A validated 1H NMR method for the determination of the degree of deacetylation of chitosan. *J Pharm Biomed Anal* 2003; 32: 1149–1158.
29. Espartero JL, Rashkov I, Li SM, et al. NMR analysis of low molecular weight poly (lactic acid). *Macromolecules* 1996; 29: 3535–3539.
30. Shabaninezhad M and Ramakrishna G. Theoretical investigation of plasmonic properties of quantum-sized silver nanoparticles. *Plasmonics* 2020; 15: 783–795.
31. Shankar SS, Rai A, Ahmad A, et al. Rapid synthesis of Au, Ag, and bimetallic Au core-Ag shell nanoparticles using Neem (Azadirachta indica) leaf broth. *J Colloid Interf Sci* 2004; 275: 496–502.
32. Holzwarth U and Gibson N. The Scherrer equation versus the 'Debye-Scherrer equation'. *Nat Nanotechnology* 2011; 6: 534.
33. Abdelgawad AM, Hudson SM and Rojas OJ. Antimicrobial wound dressing nanofiber mats from multicomponent (chitosan/silver-NPs/polyvinyl alcohol) systems. *Carbohydr Polym* 2014; 100: 166–178.
34. Rumble JR. *CRC Handbook of Chemistry and Physics*. 100th ed.. Boca Raton: (EUA)Taylor and Francis Group, 2019.
35. Ahmed M, Ramos TA, Damanik F, et al. A combinatorial approach towards the design of nanofibrous scaffolds for chondrogenesis. *Scientific Rep* 2015; 5: 14804–14812.
36. Xu LC and Siedlecki CA. Effects of surface wettability and contact time on protein adhesion to biomaterial surfaces. *Biomaterials* 2007; 28: 3273–3283.
37. Daraeinejad Z and Shabani I. Enhancing cellular infiltration on fluffy polyaniline-based electrospun nanofibers. *Front Bioeng Biotechnol* 2021; 9: 641371–641413.
38. Ameer JM, Pr AK and Kasoju N. Strategies to tune electrospun scaffold porosity for effective cell response in tissue engineering. *J Funct Biomater* 2019; 10: 30.
39. Kumar R and Münstedt H. Silver ion release from antimicrobial polyamide/silver composites. *Biomaterials* 2005; 26: 2081–2088.

40. Zou XH, Jiang YZ, Zhang GR, et al. Specific interactions between human fibroblasts and particular chondroitin sulfate molecules for wound healing. *Acta Biomater* 2009; 5: 1588–1595.
41. Frantz C, Stewart KM and Weaver VM. The extracellular matrix at a glance. *J Cel Sci* 2010; 123: 4195–4200.
42. Denuzière A, Ferrier D and Domard A. Interactions between chitosan and glycosaminoglycans (chondroitin sulfate and hyaluronic acid): Physicochemical and biological studies. *Ann pharmaceutiques francaises* 1999; 58: 47–53.
43. Tomic-Canic M, Burgess JL, O'Neill KE, et al. Skin microbiota and its interplay with wound healing. *Am J Clin Dermatol* 2020; 21: 36–43.
44. Bessa LJ, Fazii P, Di Giulio M, et al. Bacterial isolates from infected wounds and their antibiotic susceptibility pattern: Some remarks about wound infection. *Int Wound J* 2013; 12: 47–52.
45. Brown S, Santa Maria JP Jr and Walker S. Wall teichoic acids of Gram-positive bacteria. *Annu Rev Microbiol* 2013; 67: 313–336.
46. Dakal TC, Kumar A, Majumdar RS, et al. Mechanistic basis of antimicrobial actions of silver nanoparticles. *Front Microbiol* 2016; 7: 1831–1917.
47. Cui W, Zhu X, Yang Y, et al. Evaluation of electrospun fibrous scaffolds of poly (dl-lactide) and poly (ethylene glycol) for skin tissue engineering. *Mater Sci Eng C* 2009; 29: 1869–1876.
48. Zhong S, Teo WE, Zhu X, et al. Formation of collagen−glycosaminoglycan blended nanofibrous scaffolds and their biological properties. *Biomacromolecules* 2005; 6: 2998–3004.